

Brain mechanisms underlying the emotion processing bias in treatment-resistant depression

Received: 30 August 2023

Accepted: 15 March 2024

Published online: 16 April 2024

 Check for updates

Xiaoxu Fan¹, Madaline Mocchi¹, Bailey Pascuzzi¹, Jiayang Xiao¹, Brian A. Metzger², Raissa K. Mathura¹, Carl Hacker³, Joshua A. Adkinson¹, Eleonora Bartoli¹, Salma Elhassa¹, Andrew J. Watrous¹, Yue Zhang¹, Anusha Allawala⁴, Victoria Pirtle¹, Sanjay J. Mathew¹, Wayne Goodman¹, Nader Pouratian⁵ & Kelly R. Bijanki¹✉

Depression is associated with a cognitive bias towards negative information and away from positive information. This biased emotion processing may underlie core depression symptoms, including persistent feelings of sadness and a reduced capacity to experience pleasure. The neural mechanisms responsible for this biased emotion processing remain unknown. Here we had a unique opportunity to record stereotactic electroencephalography signals in the amygdala and prefrontal cortex (PFC) from 5 patients with treatment-resistant depression (TRD) and 12 patients with epilepsy (as control) while they participated in an affective bias task in which happy and sad faces were evaluated. First, compared with the control group, patients with TRD showed increased amygdala responses to sad faces in the early stage (around 300 ms) and decreased amygdala responses to happy faces in the late stage (around 600 ms) following the onset of faces. Furthermore, during the late stage of happy-face processing, alpha-band activity in the PFC as well as alpha-phase locking between the amygdala and the PFC were significantly greater in patients with TRD compared with the control group. The increased amygdala activation during the early stage of sad-face processing suggests an overactive bottom-up processing system in TRD. Meanwhile, the reduced amygdala response during the late stage of happy-face processing could be attributed to increased top-down inhibition by the PFC through alpha-band oscillation, which may be relieved following deep brain stimulation in the subcallosal cingulate and the ventral capsule/ventral striatum.

Major depressive disorder (MDD) is characterized by excessive low mood and a reduced capacity to experience pleasure. According to Beck's cognitive model of depression, the biased acquisition and processing of information have a central role in the development and

maintenance of depression^{1,2}. Numerous studies have shown that individuals with depression tend to have a negative bias across various cognitive domains, including perception^{3,4}, attention⁵ and memory⁶. For example, individuals with depression tend to interpret neutral

¹Baylor College of Medicine, Houston, TX, USA. ²Swarthmore College, Swarthmore, PA, USA. ³School of Medicine, Washington University, Saint Louis, MO, USA. ⁴University of California San Francisco, San Francisco, CA, USA. ⁵University of Texas Southwestern Medical Center, Dallas, TX, USA.

✉e-mail: bijanki@bcm.edu

Table 1 | Number of recording contacts in each patient

	Patient	Left		Right	
		PFC	Amygdala	PFC	Amygdala
TRD	Dep1	21	4	26	5
	Dep2	19	3	27	–
	Dep3	16	5	14	4
	Dep4	11	4	10	4
	Dep5	16	4	20	3
Control	EP1	9	2	–	–
	EP2	–	–	12	4
	EP3	–	5	8	–
	EP4	8	5	–	–
	EP5	–	5	–	5
	EP6	9	4	2	4
	EP7	15	2	9	–
	EP8	–	–	13	2
	EP9	–	5	11	–
	EP10	–	6	–	3
	EP11	5	–	–	–
	EP12	9	–	9	–

faces as sad, and happy faces as less happy⁷. Understanding the neural mechanism responsible for the biased processing of emotional stimuli in depression might bring important clinical benefits, including predicting, detecting and treating depression.

The biased processing of emotional stimuli in depression has been linked to dysfunction in the amygdala^{8,9}, the prefrontal cortex (PFC)^{10,11}, the dorsal anterior cingulate^{12,13} and their connections^{14,15}. Researchers have proposed that cognitive biases in depression are due to maladaptive bottom-up processes that can alter perceptions of the environment and social interactions^{16,17}. Consistent with this hypothesis, functional MRI (fMRI) studies have indicated that individuals with depression show potentiated amygdala reactivity to sad faces and reduced responsiveness to happy faces, even in the absence of conscious awareness of the picture, suggesting automatic mood-congruent cognitive biases in depression^{18,19}. However, a correlation between this automatic amygdala response and current depression severity was observed only when processing happy faces, but not sad faces¹⁸. One possibility is that there are separate neural mechanisms that increase the salience of negative stimuli and decrease the salience of positive or rewarding stimuli in depression. The reduced responsiveness of the amygdala to happy faces in individuals with depression could be due to the overregulation of the amygdala by the PFC^{16,20,21}. Consistent with this hypothesis, an fMRI study using dynamic causal modelling found increased suppressive influences from the orbitomedial prefrontal cortex to the amygdala during classification of happy faces in depression²². However, in other fMRI studies, individuals with depression showed a widespread reduction in the functional connectivity between the amygdala and the PFC^{14,23}. In some studies, researchers even proposed that decreased PFC activity reduces nucleus accumbens and amygdala reactivity in people with depression, which, in turn, contributes to the inability to adaptively alter reward-seeking behaviour^{24–26}. Owing to the predominant use of methods with either high spatial and poor temporal resolution (for example, fMRI) or high temporal and poor spatial resolution (for example, electroencephalography (EEG) and magnetoencephalography) in previous studies, the neural mechanism responsible for the biased processing of emotional stimuli in depression is far from fully understood. Here we use human intracranial stereotactic EEG (sEEG) recordings with high spatial and temporal resolution to investigate the

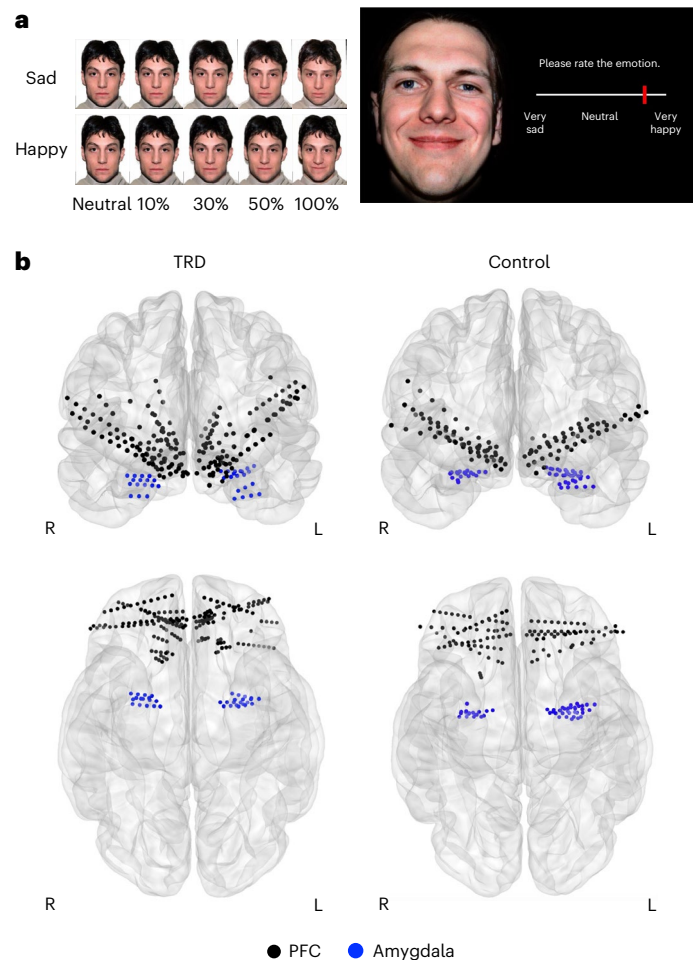


Fig. 1 | Experiment design and recording contact distribution. **a**, Affective bias task. The stimulus set includes morphed faces from maximal emotional intensity to neutral (100% sad, 50% sad, 30% sad, 10% sad, neutral, 10% happy, 30% happy, 50% happy and 100% happy). Participants were asked to rate the emotional intensity of each stimulus presented on the screen by clicking a location on the slider bar. **b**, Spatial distribution of recording contacts across 5 patients with TRD and 12 control patients in the MNI space. Top: coronal view. Bottom: inferior view. Contacts within the PFC are black and contacts within the amygdala are blue. L, left; R, right. Only contacts in the PFC and the amygdala are shown.

neurobiological mechanisms that contribute to the selective processing towards negative and away from positive stimuli in individuals with treatment-resistant depression (TRD).

Results

We recorded local field potentials from the PFC (total of 180 contacts in the TRD group and 119 contacts in the control group) and the amygdala (36 contacts in the TRD group and 52 contacts in the control group; Table 1 and Fig. 1b) in 5 patients with TRD and 12 patients with epilepsy while they participated in the affective bias task in which happy and sad faces are rated (Fig. 1a). Patients with epilepsy are here viewed as the control group, because they represented a convenience cohort who have electrodes implanted inside the brain and do not have TRD.

Temporal dynamics of amygdala responses in TRD

Given the central role of the amygdala in detecting and interpreting emotion information, we first examined the intracranial event-related potential (iERP) in the amygdala while participants rated sad and happy faces. The left, right and bilateral amygdala iERP responses to emotional faces from the two groups are shown in Fig. 2a. In each group and each

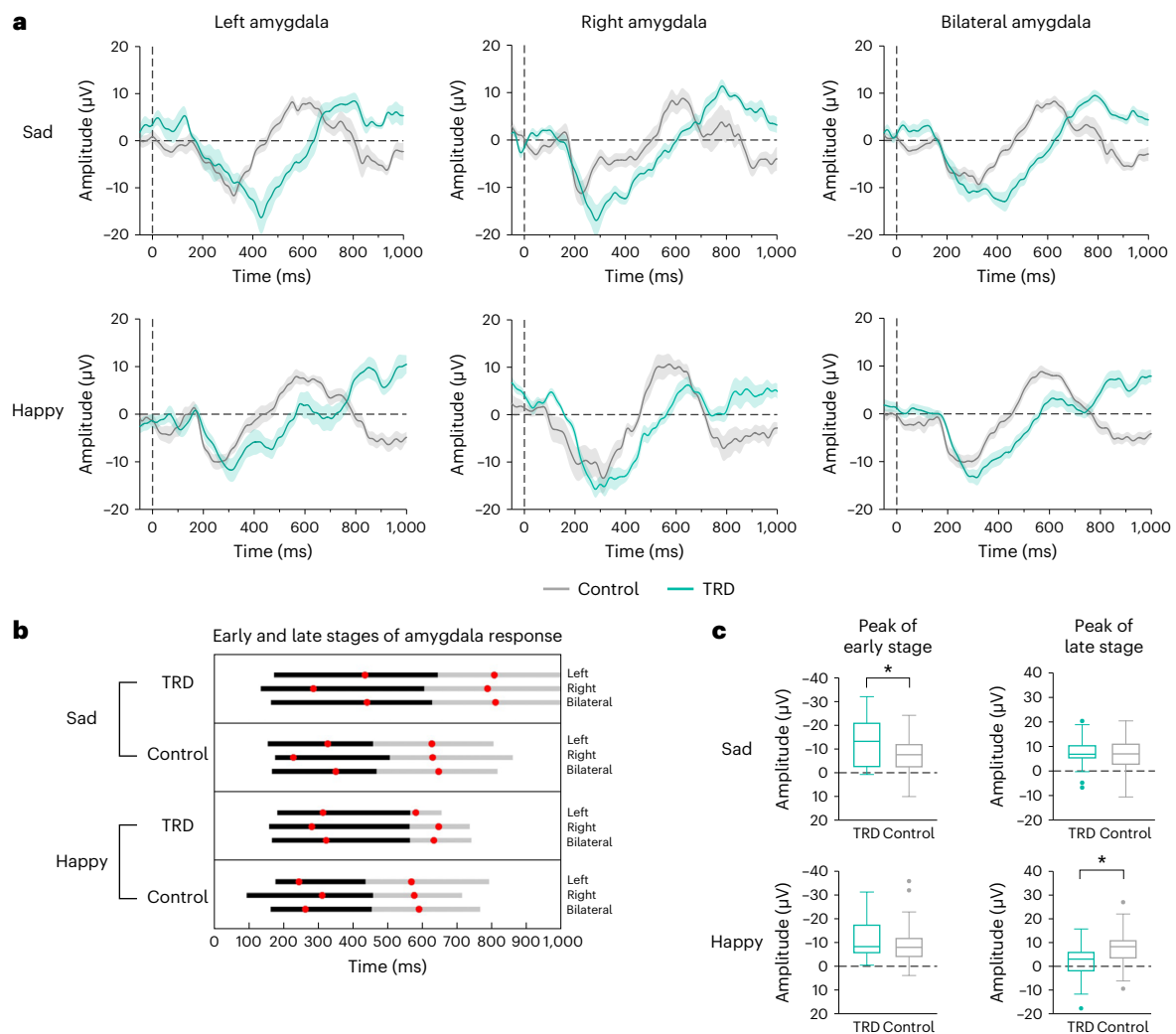


Fig. 2 | Amygdala iERP response to sad and happy faces. a, Amygdala iERPs from 5 patients with TRD (20 contacts in left amygdala and 16 contacts in right amygdala) and 12 control patients (34 contacts in left amygdala and 18 contacts in right amygdala) to sad and happy faces were averaged across contacts. The shaded area indicates s.e.m. **b**, Time windows of early-stage (black horizontal bars) and late-stage (grey horizontal bars) amygdala iERP response. The red dot depicts the time point of the average peak amplitude. **c**, Peak amplitude differences in bilateral amygdala between the TRD and control groups within the early stage and the late stage for each condition (sad and happy faces).

The centre line indicates the median, and the bottom and top edge of the box indicates the 25th and 75th percentiles, respectively. The whiskers indicate $1.5 \times$ the interquartile range up to the minimum and maximum, and the points indicate outliers. The peak amplitude of the early stage was significantly larger in the TRD group compared with the control group during sad-face processing ($t_{86} = 2.695$, $P = 0.009$). The peak amplitude of the late stage was significantly smaller in patients with TRD compared with the control group in the happy-face condition ($t_{84} = 3.610$, $P = 0.001$). * $P < 0.05$ (two-sided unpaired t -tests).

condition, there is a large negative potential peaking around 300 ms followed by a small positive potential. We define the duration of the large negative potential as the early stage of amygdala response and the small positive potential as the late stage of amygdala response (Fig. 2b). In all conditions (sad and happy), the early stage of amygdala response lasts longer in the TRD group compared with control group. Then, we calculated the peak amplitude of each stage in each group and each condition. We combined results from the left and right amygdala because similar results were obtained. The peak amplitude of the early stage was significantly larger in the TRD group compared with the control group during sad-face processing (Fig. 2c; TRD -12.9 ± 1.7 ; control -7.5 ± 1.1 ; $t_{86} = 2.695$, $P = 0.009$), but not during rating happy faces (Fig. 2c; TRD -11.0 ± 1.3 ; control -8.4 ± 1.1 ; $t_{84} = 1.567$, $P = 0.121$). Moreover, the peak amplitude of the late stage was significantly smaller in patients with TRD compared with the control group in the happy-face condition, but not in sad-face condition (Fig. 2c; happy faces: TRD 1.9 ± 1.2 ; control 7.6 ± 1.0 ; $t_{84} = 3.610$, $P = 0.001$; sad faces: TRD 7.6 ± 1.0 ; control 6.7 ± 1.0 , $t_{86} = 0.651$, $P = 0.517$). Thus, compared with the control group,

patients with TRD showed increased amygdala response to sad faces at an early latency and decreased amygdala response to happy faces at a late latency.

TRD shows greater alpha-band power in PFC at the late stage

The altered amygdala response we observed in patients with TRD could be due to the regulation from the PFC. Previous EEG studies have reported altered cortical brain network in the alpha frequency band in MDD²⁷. Here we examined whether alpha-band power (8–12 Hz) in the PFC, which may reflect excessive inhibitory processes^{28–32}, is enhanced or reduced in TRD at the early or late stages. A three-way analysis of variance (ANOVA) revealed significant main effects of emotion category (sad versus happy, $F_{(1,297)} = 17.67$, $P < 0.001$), time window (early versus late, $F_{(1,297)} = 29.51$, $P < 0.0001$) and patient group (TRD versus control, $F_{(1,297)} = 8.230$, $P = 0.0044$). The significant interactions of time window by patient group ($F_{(1,297)} = 16.98$, $P < 0.0001$) indicated that group difference was not the same at different time windows. Subsequently, Sidak's multiple comparisons test showed significant

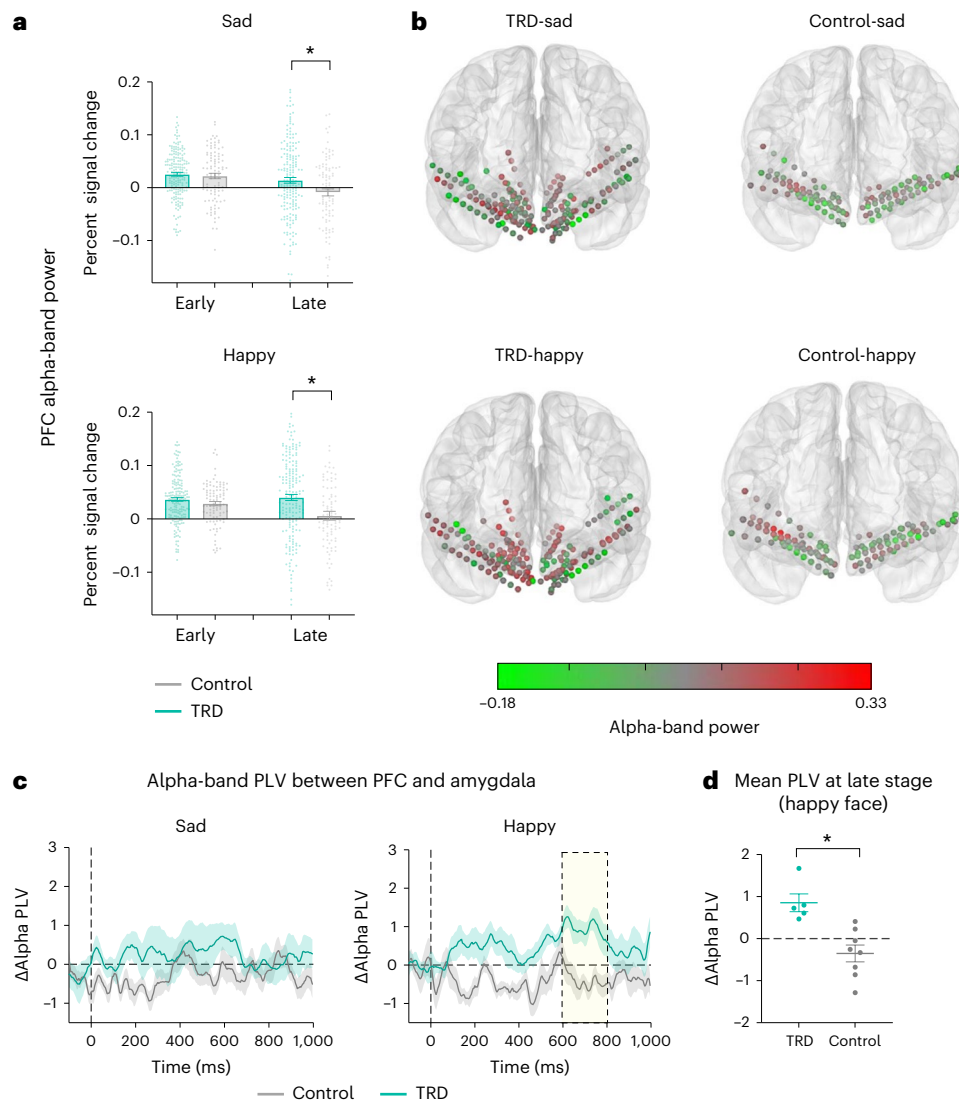


Fig. 3 | Alpha-band activity. **a**, Averaged alpha-band power in the PFC across 180 contacts in the TRD group and 119 contacts in the control group. Data are presented as mean \pm s.e.m. Sidak's multiple comparisons test showed significant differences between the TRD and control groups at the late stage of happy-face (adjusted $P < 0.0001$) and sad-face (adjusted $P = 0.0325$) processing. * $P < 0.05$. **b**, Coronal view of the alpha-band power (percent signal change) of contacts within the PFC for each group and each condition in the time window of the late stage (control-sad, 467–815 ms; control-happy, 453–765 ms; TRD-sad, 627–1000 ms; TRD-happy, 563–740 ms). Each circle represents a single contact. The percent signal changes in **a** and **b** are with respect to the pre-stimulus baseline

(–500 ms to 0 ms). **c**, Average time courses (mean \pm s.e.m.) of alpha-band PLV changes from baseline in the TRD group (5 patients) and the control group (8 patients). The yellow shaded area indicates the time window in which responses to each stimulus type (sad and happy faces) are significantly different between the TRD and the control groups with a cluster threshold of $P < 0.05$. **d**, During the late stage of happy-face processing, patients with TRD showed a stronger PLV between the PFC and amygdala than control patients ($t_{11} = 3.953$, $P = 0.0023$). Data are presented as mean \pm s.e.m. Each dot indicates a single participant. * $P < 0.05$ (two-sided unpaired t -tests). $N_{\text{TRD}} = 5$, $N_{\text{control}} = 8$.

differences between the TRD and control groups at the late stage of happy-face (adjusted $P < 0.0001$) and sad-face (adjusted $P = 0.0325$) processing (Fig. 3a). In summary, our results showed that there is no difference in PFC alpha-band power between the TRD and the control groups at the early stage. However, at the late stage, patients with TRD showed significantly greater alpha-band power in the PFC than the control group, no matter which emotional faces (sad or happy) were processed. The distribution of alpha-band power at the late stage in each group is shown in Fig. 3b.

Increased alpha amygdala–PFC synchrony in TRD

Given the increased PFC alpha-band power and decreased amygdala iERP response at the late stage of rating happy faces in the TRD group, we further hypothesized that the inhibition from the PFC to the amygdala is increased in the TRD group at the late stage of processing happy

faces. To study this hypothesis, we measured changes in the phase-locking value (PLV) of alpha oscillations between the amygdala and the PFC during sad-face and happy-face processing, which is a measure of connectivity between two regions. Only a subset of patients ($N_{\text{TRD}} = 5$, $N_{\text{control}} = 8$) with at least one contact in both the amygdala and the PFC were involved in this data analysis. The TRD group showed a greater PLV during happy-face trials than the control group from 608 ms to 792 ms (Fig. 3c; cluster-based permutation test with a cluster threshold $P < 0.05$). No time cluster expressing a significant group difference was observed in the sad-face condition (Fig. 3c). In addition, we calculated the mean PLV within the late stage of happy-face processing, and the results showed that the alpha-band PLV between the PFC and amygdala is significantly higher in the TRD group than in the control group (Fig. 3d; unpaired t -test, $t_{11} = 3.953$, $P = 0.0023$). To exclude the possibility that the increased PLV in the TRD group is due to the larger number of

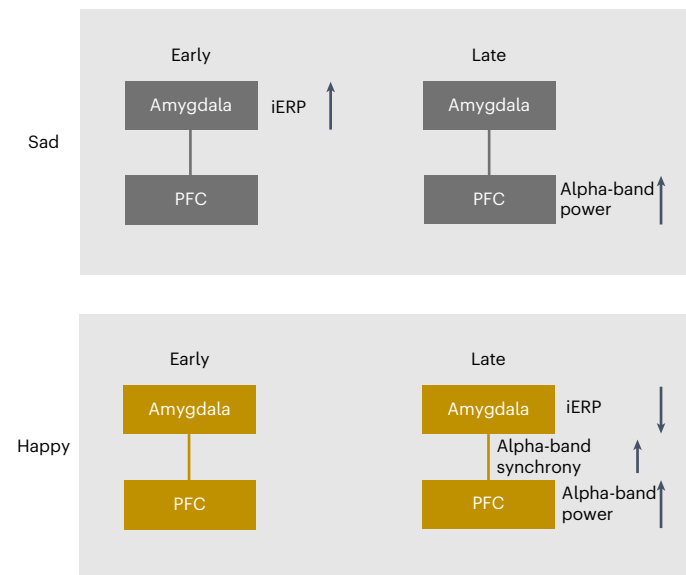


Fig. 4 | Summary of the results in patients with TRD. The arrows indicate higher or lower signal in the TRD group than in the control group.

contacts in the TRD group than in the control group, we matched the number of contacts in the two groups and calculated the PLV as before. Specifically, we randomly selected 5 contacts in the amygdala and 11 contacts in the PFC in each patient with TRD to reduce the number of total contacts involved in the PLV analysis. The same results were observed after matching the number of contacts in the TRD and the control group (Extended Data Fig. 1).

In summary, our results revealed separate neural mechanisms for the biased processing of emotional stimuli in TRD (Fig. 4). When individuals with TRD process sad faces, they show a larger amygdala iERP response at the early stage than control individuals. While processing happy faces, patients with TRD show a decreased amygdala iERP response, increased alpha-band power in the PFC and enhanced alpha-band synchrony between these two regions at the late stage, compared with the control group.

Deep brain stimulation altered the neural responses to emotional stimuli in the TRD group

All five patients with TRD were asked to perform the affective bias task again after receiving deep brain stimulation (DBS) in the subcallosal cingulate (SCC) and the ventral capsule/ventral striatum (VC/VS) (Fig. 5a). We recorded and analysed local field potentials from sEEG contacts in the PFC and amygdala as before. First, amygdala iERP responses to sad and happy faces were significantly increased after DBS in a late time window (Fig. 5b; sad, 563–713 ms; happy, 598–796 ms; cluster-based permutation test with cluster threshold $P < 0.05$). The shape of the early-stage amygdala iERP response was not changed by DBS. Second, the alpha-band power in the PFC was significantly reduced after DBS in both the early and late stages when patients with TRD process happy faces (Fig. 5c; TRD pre-DBS happy early versus TRD post-DBS happy early, adjusted $P < 0.001$; TRD pre-DBS happy late versus TRD post-DBS happy late, adjusted $P < 0.001$). Interestingly, patients with TRD did not show changed alpha-band power in the PFC at any stage in the sad-face condition (Fig. 5c; TRD pre-DBS sad early versus TRD post-DBS sad early, adjusted $P = 0.993$; TRD pre-DBS sad late versus TRD post-DBS sad late, adjusted $P = 0.9474$). Third, in the happy-face condition, the PLV was reduced to an intermediate pattern between TRD pre-DBS and the control group. Overall, after DBS in the SCC and VC/VS, the amygdala iERP response, PFC alpha-band power and the PLV between the amygdala and PFC during the processing of happy faces in patients with TRD looked more like those observed in the control group.

Discussion

With the help of the excellent spatial and temporal resolution of sEEG, we observed that increased amygdala responses to sad faces emerged at an early stage (around 300 ms), while decreased amygdala responses to happy faces emerged at a late stage (around 600 ms). Importantly, during this late stage of decreased amygdala responses to happy faces, we found increased alpha-band activity in the PFC, as well as greater alpha-phase locking between the amygdala and the PFC in patients with TRD compared with the controls. After the delivery of stimulation to two hubs that connect cortical and subcortical network regions relevant to the expression of depressive symptoms, the atypical amygdala and PFC activity, along with their connections while rating happy faces in patients with TRD looked more like those observed in the control group. Thus, our results provide important direct electrophysiological evidence for the neural mechanisms underlying the biased processing of emotional stimuli in depression. The increased amygdala iERP response during the early stage of rating sad faces suggests an overactive bottom-up processing system. While the reduced amygdala iERP response during the late stage of rating happy faces may be attributed to increased top-down inhibition by the PFC through alpha-band oscillation.

The amygdala has a critical role in emotion processing and response. It interacts with a variety of cortical and subcortical areas, which together evaluate the salience of sensory stimuli and modify the response of the amygdala³³. Numerous fMRI studies have shown that individuals with depression show an increased amygdala response to sad faces and a decreased amygdala response to happy faces compared with healthy controls^{8,19,34}. Our iERP results clearly showed that patients with TRD showed heightened and prolonged amygdala activity in response to sad faces, compared with the control group. More interestingly, the iERP traces from patients with TRD and the control patients are almost overlapping before 200 ms, suggesting no difference in the initial response to sad faces in the amygdala. This finding aligns with the theory that individuals with and without depression do not primarily differ in their initial response to negative events but in their ability to recover from the ensuing negative affect³⁵. In addition, we also observed prolonged activity in the amygdala during the early stage of happy-face processing, although without a significant change in amplitude compared with the controls. Overall, the longer-lasting amygdala response observed in our study could be related to the extended elaborative processing of emotional information in depression³⁶.

The increased amygdala iERP we observed at the early stage during sad-face processing in the TRD group supports the hypothesis that increased amygdala activity creates a bottom-up signal that biases negative information processing in higher cortical areas and can maladaptively alter perceptions of the environment¹⁹. The altered perception of negative information has been associated with decreased cognitive control from the dorsolateral prefrontal cortex^{20,37,38}. Another possibility could be that the reduced connectivity between the thalamus and dorsal anterior cingulate cortex leads to a higher flow of information through the subgenual cingulate cortex. This, in turn, heightens the emotional impact of incoming stimuli for individuals with depression^{3,12}. As individuals with depression often show an attentional bias for sad stimuli⁵, it is still unclear how the increased amygdala response to negative stimuli is related to the inefficient attentional disengagement from negative stimuli.

In the current study, patients with TRD show decreased amygdala response, increased alpha-band power in the PFC and enhanced alpha synchrony between these two regions at the late stage of happy-face processing, compared with the control group. Thus, the reduced amygdala response to happy faces in the TRD group could be due to the inhibition from the PFC. Consistent with our findings, an fMRI study examined the functional connectivity between the amygdala and orbitomedial prefrontal cortex using dynamic causal modelling,

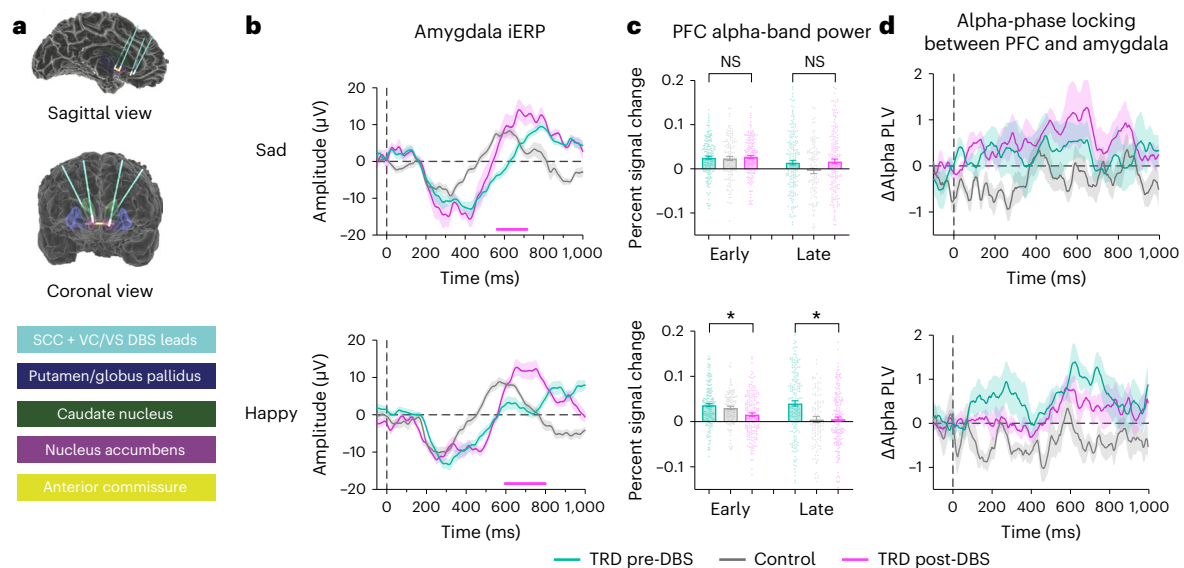


Fig. 5 | Neural responses altered by DBS. **a**, Schematic of DBS leads placement in 5 patients with TRD. **b–d**, Data from the control group are shown again here as a reference (grey), but not included in the statistical analysis. **b**, Amygdala iERP responses to sad and happy faces were averaged across contacts for each group (TRD pre-DBS, control and TRD post-DBS). The pink horizontal bar below means significant difference between TRD pre-DBS and TRD post-DBS. The shaded area indicates s.e.m. **c**, Averaged alpha-band power in the PFC across contacts. A three-way ANOVA revealed significant main effects of DBS (pre versus post,

$F_{(1,179)} = 20.14, P < 0.0001$), significant interactions of DBS effect by emotion category ($F_{(1,179)} = 26.69, P < 0.0001$) and stage ($F_{(1,179)} = 9.209, P = 0.0028$). Sidak's multiple comparisons test showed significant differences between TRD pre-DBS and TRD post-DBS at the early (adjusted $P < 0.0001$) and late (adjusted $P < 0.0001$) stages of happy-face processing. *Adjusted $P < 0.05$. Data are presented as mean \pm s.e.m. Each dot indicates a single contact ($N_{\text{TRD}} = 180$; $N_{\text{control}} = 119$). **d**, Averaged time courses (mean \pm s.e.m.) of alpha-band PLV changes from baseline across participants (TRD pre-DBS, control and TRD post-DBS).

and identified increased negative left-sided top-down orbitomedial prefrontal cortex–amygdala effective connectivity in response to happy faces²². The connectivity results suggest increased inhibition of the left amygdala by the left orbitomedial prefrontal cortex in response to positive emotional stimuli. In addition, increased alpha-band power in the PFC of individuals with depression has been reported in previous EEG studies^{27,39,40}. This heightened alpha activity may reflect excessive inhibitory processes, which could contribute to the cognitive and emotional symptoms associated with depression. Consistent with this idea, a clinical improvement after antidepressant treatments was also found to be associated with a decrease in PFC alpha-band activity^{41,42}.

With the help of the high temporal and spatial resolution of intracranial EEG, our results support that separate neural mechanisms are responsible for the biased negative and positive affective information processing in depression. The observed effect of DBS also provides evidence for this hypothesis. Specifically, after DBS in the SCC and VC/VS, both the alpha-band power in the PFC and the alpha-band PLV between the PFC and amygdala during happy-face processing were reduced. However, DBS has little effect on PFC alpha-band power and alpha-band PLV between the PFC and amygdala during sad-face processing. Consistent with our results, decreased positive emotion rather than exaggerated responses to negative stimuli is thought to be a distinctive feature of depression. For example, amygdala activity during happy-face processing or positive recall was negatively correlated with current depression severity^{18,43}. But no significant correlation between amygdala activity during sad-face processing and current depression severity was observed in those studies. Also, it is worth noting that a negative processing bias also exists in high-risk populations of depression and individuals with anxiety^{43,44}. Similarly, some studies have proposed that amygdala hyperactivity during negative autobiographical recall is a trait-like marker of depression, while amygdala hypoactivity during positive autobiographical recall is a state marker that emerges during active disease and returns to normal with symptom remission⁴³.

Converging evidence suggests an important role of amygdala in the recovery from MDD. In some studies, individuals with MDD have

been trained to regulate their amygdala haemodynamic response during real-time fMRI neurofeedback training⁴⁵. After training, the amygdala haemodynamic response to positive memories or happy faces was increased and depressive symptoms were reduced, suggesting a recovery from depression. In patients with MDD after sertraline treatment, hyperactivation of the amygdala to masked sad faces decreased and hypoactivation of the amygdala to masked happy faces increased¹⁹. Consistent with these findings, our results also showed that the processing bias of happy faces looks more like the control group after DBS. Together with previous findings, the decreased activation of the amygdala to positive stimuli may indicate clinical significance and some antidepressant drugs or cognitive therapies exert their treatment effect by normalizing this emotional processing.

Intracranial recordings in patients with TRD before and after DBS parameter exploration allowed this extraordinary opportunity to study the neural mechanism of biased processing of emotional stimuli in depression, but some limitations must be acknowledged. For example, we use patients with epilepsy as the control group in our study because it is impossible to get sEEG data from healthy humans. Patients with epilepsy often show a range of depressive comorbidities⁴⁶; however, none of the patients included in this study was diagnosed with TRD. Although the 12 patients with epilepsy used as the control group showed a range of depression from minimal to severe, we have identified a significant difference between the TRD and control groups. If there is a control group in which all participants have completely no depression, we would get same conclusion but with larger difference and stronger statistical power. Another limitation is that a conclusive behavioural result was not obtained due to the small number of patients with TRD involved in our study. Unlike intracranial EEG data in which multiple electrodes are placed inside the brain to record electrical activity directly, an adequate sample size of patients is necessary for a conclusive behavioural result, especially when comparing between groups. However, there is substantial behavioural evidence showing that individuals with MDD show blunted responsiveness to happy faces and an increased tendency to interpret neutral faces as sad^{47–50}. The

increased amygdala iERP response to sad faces and decreased amygdala iERP response to happy faces observed in our study are consistent with these previously reported negative cognitive bias in depression. The third limitation is that the spatial coverage of electrodes in patients with TRD in the frontal lobe is limited with respect to the epilepsy cohort due to differences in the surgical targets, driven uniquely by clinical purposes. As a consequence, our ability to resolve the contribution of different PFC subdivisions was not possible in the current study, and further evidence is needed to pinpoint the exact source of the PFC inhibitory effects. Nonetheless, our results investigated the functional profile of amygdala, PFC and their connectivity in affective processing and provide direct electrophysiological evidence with high spatial and temporal resolution to understand the critical framework for the biased acquisition and processing of information, which has a primary role in the development and maintenance of depression.

Methods

Participants

Data were obtained from 12 patients with epilepsy (7 female, 5 male, age 19–57) and 5 patients with TRD (3 female, 2 male, age 32–56). Twelve patients with epilepsy were undergoing sEEG monitoring at Baylor College of Medicine for seizure localization before surgical resection. All participants with epilepsy completed questionnaires on depressive symptoms (Beck Depression Inventory-II (BDI-II)⁵¹) and their BDI-II scores show a distribution from minimal to severe depression (Extended Data Fig. 2). The average BDI-II score was 21.17 ± 11.7 (mean \pm s.d.). Participants with TRD involved in this study ($N = 5$) were enrolled in an early feasibility trial (ClinicalTrials.gov Identifier: [NCT03437928](https://clinicaltrials.gov/ct2/show/study/NCT03437928)) of individualized DBS guided by intracranial recordings⁵². All five patients with TRD have a DSM-5⁵³ diagnosis of MDD as their primary diagnosis and failed to respond to a minimum of four adequate depression treatments from at least two different treatment medication categories (selective serotonin reuptake inhibitors, serotonin and norepinephrine reuptake inhibitors, tricyclic antidepressant, monoamine oxidase inhibitors, and so on). One week before operation in patients with TRD, MADRS (Montgomery–Asberg Depression Rating Scale) and HAM-D (Hamilton Depression Rating Scale) were administered by the clinician to assess the severity of depression. All patients with TRD had a MADRS score above 27 and a HAM-D score above 20. Participants with history of psychosis, personality disorder, recent suicide attempt or neurodegenerative disorders were excluded from recruitment. Each patient with TRD was implanted with ten temporary sEEG electrodes for neural recordings and four permanent DBS leads for stimulation delivery (DBS leads are shown in Fig. 5a and Extended Data Fig. 3a). sEEG electrodes in patients with TRD were used to conduct a thorough search of stimulation parameter space to build a comprehensive understanding of the pathophysiology of TRD, as well as the neural responses to stimulation therapy⁵². This clinical trial is funded by the NIH Brain Research Through Advancing Innovative Neurotechnologies (BRAIN) Initiative (UH3 NS103549) and approved by the Food and Drug Administration (IDE number G180300). All the experiments in this paper involving patients with epilepsy and patients with TRD were approved by the institutional review board at Baylor College of Medicine (IRB: H-43036, IRB: H-18112). Written informed consent was obtained from each participant. The patients were paid US\$100 per day.

Electrode implantation and localization

DBS leads (Cartesia, Boston Scientific) and sEEG electrodes (Depthlon, PMT) were implanted using a robotic surgical assistant (Zimmer Biomet). The locations of sEEG electrodes in patients with epilepsy were entirely based on medical considerations (detection of the seizure foci). Each 0.8-mm-diameter sEEG electrode contains 12–16 independent recording contacts. Contacts (2 mm in length) are spaced 1.5 mm apart from one another, edge to edge. All patients with epilepsy involved

in our study have at least one electrode in the PFC or amygdala. Each patient with TRD had ten sEEG electrodes (five per hemisphere in the prefrontal and mesial temporal regions) and four DBS leads (VC/VS and SCC bilaterally). The surgery procedure and DBS leads information can be found in a previously published study⁵². Following surgical implantation, electrodes were localized by co-registration of pre-surgery anatomical T1MRI scans and post-implantation computed tomography scans using FreeSurfer Version 6 (<https://surfer.nmr.mgh.harvard.edu>). Electrode positions were manually marked using BiImage Suite⁵⁴. iELVis⁵⁵ was used to overlay electrode location into the MRI. Electrodes were then assigned to the PFC and amygdala by independent expert visual inspection. We projected electrode positions onto Montreal Neurological Institute-152 template brain (MNI) space and displayed on the cortical surface of FreeSurfer 'fsaverage' brain for visualization in Fig. 1b.

Affective bias task

Participants in our study were asked to rate emotional human face photographs, which were displayed on a Viewsonic VP150 monitor with a resolution of $1,920 \times 1,080$, positioned 57 cm from the participants. Happy, sad and neutral face exemplars (6 identities each; 3 male, 3 female) adapted from the NimStim Face Stimulus Set⁵⁶ were morphed using a Delaunay tessellation matrix to generate subtle facial expressions ranging in emotional intensity from neutral to maximally expressive in steps of 10%, 30%, 50% and 100% for happy and sad faces, respectively (Fig. 1a). The experiment was programmed in MATLAB R2019a, using Psychtoolbox-3⁵⁷.

In each trial, a white fixation cross was displayed on a black background for 1,000 ms (jittered \pm 100 ms) and then a face and a rating prompt appeared simultaneously on the screen, positioned on the left and right sides, respectively (as illustrated in Fig. 1a). Participants were asked to indicate their rating by clicking a specific location on the slider bar using a computer mouse. The ratings were recorded using a continuous scale that ranged from 0 ('Very sad') to 0.5 ('Neutral') to 1 ('Very happy'). Stimuli were presented in a blocked design in which all happy faces (plus neutral) appeared in one block while all sad faces (plus neutral) appeared in a separate block. There were 30 trials in each block (6 trials for each intensity level). Participants completed three alternating happy and sad blocks. The order of happy and sad blocks was counterbalanced across participants. Patients with TRD underwent sEEG research for 10 days in the epilepsy monitoring unit and they performed the affective bias task twice after surgical implantation, at day 1 or day 2 (before DBS parameter exploration) and day 8 or day 9 (after DBS parameter exploration). Patients with epilepsy completed the task during their in-patient stay (at least 2 hours after any seizure activity was detected). Trials with obvious wrong clicks (for example, 100% happy faces were labelled very sad: 1.5% in control group; 1.4% in TRD group), which indicated that the patients were distracted from doing the task, were excluded from data analysis.

Data acquisition and preprocessing

Intracranial EEG data were recorded during affective bias task using Cerebus data acquisition system (Blackrock Neurotech). All neural signals were recorded at a 2,000 Hz sampling rate (online band-pass filter 0.3–500 Hz) with a 256-channel amplifier and referenced to a contact in the white matter. Some runs of patient DBSTRD010 were collected at 30 kHz for reasons pertaining to other studies and were downsampled to 2,000 Hz. A photodiode was placed in the lower right-hand corner of the screen to mark the trial onset and its analogue voltage response was recorded by the data acquisition system to ensure precise synchronization. Electrode contacts and epochs contaminated with excessive artefacts and epileptiform activity were removed from data analysis by visual inspection. After that, the continuous intracranial EEG data in each electrode contact was notch-filtered at 60 Hz, re-referenced to the common average reference and segmented from -500 ms to 1,000 ms relative to stimulus onset. Neutral face epochs in each block

were removed from data analysis. Intracranial EEG data were analysed using MNE-Python⁵⁸ v1.6 (<https://mne.tools/stable/index.html>) and MATLAB R2023a.

Quantification and statistical analysis

Event-related potentials. The segmented data were band-pass filtered from 1 Hz to 30 Hz using a finite impulse response filter (MNE-Python⁵⁸). iERPs were calculated for each condition (happy and sad), each group (TRD, control) and each contact by averaging the filtered epochs and normalizing them to the mean signal of baseline period (−500 ms to 0 ms relative to stimulus onset). The iERP time courses were averaged across contacts within the left amygdala, right amygdala and bilateral amygdala for each condition (Fig. 2a). The data from two contacts in patient Dep3 in happy blocks was excluded from time course and amplitude analysis as an extreme outlier (>8 s.d. away from the mean). On the basis of the averaged amygdala iERP waveform across contacts, we defined the duration of the large negative potential as the early stage of amygdala response and the small positive potential as the late stage of amygdala response. Specifically, the duration of the early and late stages of amygdala response are defined as same polarity time points surrounding the peak of negative potential and positive potential, respectively (Fig. 2b). The peak amplitude of each stage was calculated as the average amplitude within a 150 ms time window of the peak (Fig. 2c). Group differences in peak amplitude were tested with two-tailed unpaired *t*-test.

Power analysis. For each recording contact, alpha-band power was estimated for the early stage and the late stage. We band-pass filtered the data (8–12 Hz, IIR filter), applied the Hilbert transform to extract analytic amplitude envelope, squared the results and normalized them by calculating percent change from pre-stimulus baseline (−500 ms to 0 ms). The results shown in Fig. 3a were averaged across all the contacts for each group and each condition. We performed three-way ANOVA (emotion category × time window × patient group) on the alpha-band power data. Sidak's multiple comparisons test was used to estimate the differences between the TRD and control groups.

Inter-regional phase synchrony. The PLV⁵⁹ was calculated for each contact pair between the PFC and amygdala. Only a subset of patients with at least one contact in both the amygdala and the PFC were involved in data analysis ($N_{\text{TRD}} = 5$, $N_{\text{control}} = 8$). The average BDI-II score of the control group was 14.00 ± 4.23 (mean ± s.d.). The preprocessed data were alpha-band filtered (8–12 Hz) using a finite impulse response filter (order, 4 cycles of the desired signal). Then Hilbert transform was applied and the PLV was calculated for each contact pair and normalized to the baseline (−500 ms to 0 ms). The results shown in Fig. 3c were averaged across participants. For each condition (sad and happy), we statistically compared the PLVs between the TRD and control groups using a cluster-based permutation test ($N = 10,000$, cluster $P < 0.05$, Bonferroni corrected). We also compared the mean PLV of happy-face trials during the late stage (TRD, from 563 ms to 740 ms; control, from 453 ms to 765 ms) between the TRD and control groups (unpaired *t*-test).

DBS stimulation

The DBS leads were positioned to the target region (SCC and VC/VS) using previously described methodology based on patient-specific diffusion-weighted imaging data⁶⁰. DBS parameter exploration was initiated 3 days after surgery (surgery day is day 0) in patients with TRD as described in the clinical protocol (Food and Drug Administration IDE number G180300). We delivered stimulation to the target regions using different parameter sets (Cerestim, Blackrock Microsystems) from day 3 to day 8 or day 9. We tested a wide range of parameter space by varying stimulation target (left SCC, right SCC, left VC/VS, right VC/VS), frequency (6 Hz, 50 Hz, 130 Hz), amplitude (2 mA, 5 mA) and

pulse width (50 μs, 100 μs, 180 μs). We also varied the contact configuration (that is, the combination of DBS contacts through which stimulation was delivered) by separately testing the bottom bullet-shaped contact, top ring contact and three 'stacks' of segmented contacts in the middle two levels on the VC/VS leads (see Extended Data Fig. 3 for a picture of DBS lead⁶¹ and an example stimulation parameter set). For the SCC leads, we additionally tested the middle two segmented levels. We tested all combinations of these parameters across the four DBS leads⁵². After DBS parameter exploration, patients with TRD were asked to perform affective bias task again at day 8 or day 9, during which all the stimulation was turned off.

Reporting summary

Further information on research design is available in the Nature Portfolio Reporting Summary linked to this article.

Data availability

The data that support the key findings are available on Open Science Framework at <https://osf.io/93wf2/> (ref. 62). Source data are provided with this paper.

Code availability

The codes used to analyse the data of this study are publicly available on Open Science Framework at <https://osf.io/93wf2/> (ref. 62).

References

1. Beck, A. T. *Depression: Clinical, Experimental, and Theoretical Aspects* (Harper & Row, 1967).
2. Beck, A. T. The evolution of the cognitive model of depression and its neurobiological correlates. *Am. J. Psychiatry* **165**, 969–977 (2008).
3. Disner, S. G., Beevers, C. G., Haigh, E. A. P. & Beck, A. T. Neural mechanisms of the cognitive model of depression. *Nat. Rev. Neurosci.* **12**, 467–477 (2011).
4. Roiser, J. P., Elliott, R. & Sahakian, B. J. Cognitive mechanisms of treatment in depression. *Neuropsychopharmacology* **37**, 117–136 (2012).
5. Gotlib, I. H., Krasnoperova, E., Yue, D. N. & Joormann, J. Attentional biases for negative interpersonal stimuli in clinical depression. *J. Abnorm. Psychol.* **113**, 121–135 (2004).
6. Hamilton, J. P. & Gotlib, I. H. Neural substrates of increased memory sensitivity for negative stimuli in major depression. *Biol. Psychiatry* **63**, 1155–1162 (2008).
7. Bourke, C., Douglas, K. & Porter, R. Processing of facial emotion expression in major depression: a review. *Aust. N. Z. J. Psychiatry* **44**, 681–696 (2010).
8. Arnone, D. et al. Increased amygdala responses to sad but not fearful faces in major depression: relation to mood state and pharmacological treatment. *Am. J. Psychiatry* **169**, 841–850 (2012).
9. Young, K. D. et al. Randomized clinical trial of real-time fMRI amygdala neurofeedback for major depressive disorder: effects on symptoms and autobiographical memory recall. *Am. J. Psychiatry* **174**, 748–755 (2017).
10. Siegle, G. J., Thompson, W., Carter, C. S., Steinhauer, S. R. & Thase, M. E. Increased amygdala and decreased dorsolateral prefrontal BOLD responses in unipolar depression: related and independent features. *Biol. Psychiatry* **61**, 198–209 (2007).
11. Zhong, M. et al. Amygdala hyperactivation and prefrontal hypoactivation in subjects with cognitive vulnerability to depression. *Biol. Psychol.* **88**, 233–242 (2011).
12. Greicius, M. D. et al. Resting-state functional connectivity in major depression: abnormally increased contributions from subgenual cingulate cortex and thalamus. *Biol. Psychiatry* **62**, 429–437 (2007).

13. Foland-Ross, L. C. et al. The neural basis of difficulties disengaging from negative irrelevant material in major depression. *Psychol. Sci.* **24**, 334–344 (2013).
14. Ramasubbu, R. et al. Reduced intrinsic connectivity of amygdala in adults with major depressive disorder. *Front. Psychiatry* **5**, 17 (2014).
15. Cheng, W. et al. Functional connectivity of the human amygdala in health and in depression. *Soc. Cogn. Affect. Neurosci.* **13**, 557–568 (2018).
16. Kim, Y. *Major Depressive Disorder—Cognitive and Neurobiological Mechanisms* (InTech, 2015).
17. Clark, D. A. & Beck, A. T. Cognitive theory and therapy of anxiety and depression: convergence with neurobiological findings. *Trends Cogn. Sci.* **14**, 418–424 (2010).
18. Suslow, T. et al. Automatic mood-congruent amygdala responses to masked facial expressions in major depression. *Biol. Psychiatry* **67**, 155–160 (2010).
19. Victor, T. A., Furey, M. L., Fromm, S. J., Öhman, A. & Drevets, W. C. Relationship between amygdala responses to masked faces and mood state and treatment in major depressive disorder. *Arch. Gen. Psychiatry* **67**, 1128–1138 (2010).
20. Drevets, W. C. Neuroimaging and neuropathological studies of depression: implications for the cognitive-emotional features of mood disorders. *Curr. Opin. Neurobiol.* **11**, 240–249 (2001).
21. Almeida, J. R. C., Versace, A., Hassel, S., Kupfer, D. J. & Phillips, M. L. Elevated amygdala activity to sad facial expressions: a state marker of bipolar but not unipolar depression. *Biol. Psychiatry* **67**, 414–421 (2010).
22. Almeida, J. R. C. et al. Abnormal amygdala-prefrontal effective connectivity to happy faces differentiates bipolar from major depression. *Biol. Psychiatry* **66**, 451–459 (2009).
23. Dannlowski, U. et al. Reduced amygdaloprefrontal coupling in major depression: association with MAOA genotype and illness severity. *Int. J. Neuropsychopharmacol.* **12**, 11–22 (2009).
24. Heller, A. S. et al. Reduced capacity to sustain positive emotion in major depression reflects diminished maintenance of frontostriatal brain activation. *Proc. Natl Acad. Sci. USA* **106**, 22445–22450 (2009).
25. Pizzagalli, D. A. & Roberts, A. C. Prefrontal cortex and depression. *Neuropsychopharmacology* **47**, 225–246 (2022).
26. Epstein, J. et al. Lack of ventral striatal response to positive stimuli in depressed versus normal subjects. *Am. J. Psychiatry* **163**, 1784–1790 (2006).
27. Shim, M., Im, C. H., Kim, Y. W. & Lee, S. H. Altered cortical functional network in major depressive disorder: a resting-state electroencephalogram study. *NeuroImage Clin.* **19**, 1000–1007 (2018).
28. Neuper, C. & Pfurtscheller, G. Event-related dynamics of cortical rhythms: frequency-specific features and functional correlates. *Int. J. Psychophysiol.* **43**, 41–58 (2001).
29. Engel, A. K., Fries, P. & Singer, W. Dynamic predictions: oscillations and synchrony in top-down processing. *Nat. Rev. Neurosci.* **2**, 704–716 (2001).
30. Foxe, J. J. & Snyder, A. C. The role of alpha-band brain oscillations as a sensory suppression mechanism during selective attention. *Front. Psychol.* **2**, 154 (2011).
31. Jensen, O. & Mazaheri, A. Shaping functional architecture by oscillatory alpha activity: gating by inhibition. *Front. Hum. Neurosci.* **4**, 186 (2010).
32. Klimesch, W., Sauseng, P. & Hanslmayr, S. EEG alpha oscillations: the inhibition-timing hypothesis. *Brain Res. Rev.* **53**, 63–88 (2007).
33. Sander, D., Grafman, J. & Zalla, T. The human amygdala: an evolved system for relevance detection. *Rev. Neurosci.* **14**, 303–316 (2003).
34. Surguladze, S. et al. A differential pattern of neural response toward sad versus happy facial expressions in major depressive disorder. *Biol. Psychiatry* **57**, 201–209 (2005).
35. Teasdale, J. D. & Dent, J. Cognitive vulnerability to depression: an investigation of two hypotheses. *Br. J. Clin. Psychol.* **26**, 113–126 (1987).
36. Siegle, G. J., Steinhauer, S. R., Thase, M. E., Stenger, V. A. & Carter, C. S. Can't shake that feeling: event-related fMRI assessment of sustained amygdala activity in response to emotional information in depressed individuals. *Biol. Psychiatry* **51**, 693–707 (2002).
37. Fales, C. L. et al. Altered emotional interference processing in affective and cognitive-control brain circuitry in major depression. *Biol. Psychiatry* **63**, 377–384 (2008).
38. Ochsner, K. N. & Gross, J. J. The cognitive control of emotion. *Trends Cogn. Sci.* **9**, 242–249 (2005).
39. Jaworska, N., Blier, P., Fusee, W. & Knott, V. Alpha power, alpha asymmetry and anterior cingulate cortex activity in depressed males and females. *J. Psychiatr. Res.* **46**, 1483–1491 (2012).
40. Fingelkurts, A. A. et al. Impaired functional connectivity at EEG alpha and theta frequency bands in major depression. *Hum. Brain Mapp.* **28**, 247–261 (2007).
41. Ulrich, G., Renfordt, E., Zeller, G. & Frick, K. Interrelation between changes in the EEG and psychopathology under pharmacotherapy for endogenous depression. A contribution to the predictor question. *Pharmacopsychiatry* **17**, 178–183 (1984).
42. Olbrich, S. & Arns, M. EEG biomarkers in major depressive disorder: discriminative power and prediction of treatment response. *Int. Rev. Psychiatry* **25**, 604–618 (2013).
43. Young, K. D., Siegle, G. J., Bodurka, J. & Drevets, W. C. Amygdala activity during autobiographical memory recall in depressed and vulnerable individuals: association with symptom severity and autobiographical overgenerality. *Am. J. Psychiatry* **173**, 78–89 (2016).
44. Teachman, B. A., Joormann, J., Steinman, S. A. & Gotlib, I. H. Automaticity in anxiety disorders and major depressive disorder. *Clin. Psychol. Rev.* **32**, 575–603 (2012).
45. Young, K. D. et al. Real-time functional magnetic resonance imaging amygdala neurofeedback changes positive information processing in major depressive disorder. *Biol. Psychiatry* **82**, 578–586 (2017).
46. Fiest, K. M. et al. Depression in epilepsy: a systematic review and meta-analysis. *Neurology* **80**, 590–599 (2013).
47. Münkler, P., Rothkirch, M., Dalati, Y., Schmack, K. & Sterzer, P. Biased recognition of facial affect in patients with major depressive disorder reflects clinical state. *PLoS ONE* **10**, e0129863 (2015).
48. Gollan, J. K., Pane, H. T., McCloskey, M. S. & Coccaro, E. F. Identifying differences in biased affective information processing in major depression. *Psychiatry Res.* **159**, 18–24 (2008).
49. Gur, R. C. et al. Facial emotion discrimination: II. Behavioral findings in depression. *Psychiatry Res.* **42**, 241–251 (1992).
50. Liu, W., Huang, J., Wang, L., Gong, Q. & Chan, R. C. K. Facial perception bias in patients with major depression. *Psychiatry Res.* **197**, 217–220 (2012).
51. Beck, A. T., Steer, R. A. & Brown, G. K. *Manual for the Beck Depression Inventory-II* (Psychological Corporation, 1996).
52. Sheth, S. A. et al. Deep brain stimulation for depression informed by intracranial recordings. *Biol. Psychiatry* **92**, 246–251 (2022).
53. American Psychiatric Association *Diagnostic and Statistical Manual of Mental Disorders* 5th edn (Booksmith Publishing, 2021).
54. Papademetris, X. et al. BiImage suite: an integrated medical image analysis suite: an update. *Insight J.* **2006**, 209 (2006).
55. Groppe, D. M. et al. iELVis: an open source MATLAB toolbox for localizing and visualizing human intracranial electrode data. *J. Neurosci. Methods* **281**, 40–48 (2017).

56. Tottenham, N. et al. The NimStim set of facial expressions: judgments from untrained research participants. *Psychiatry Res.* **168**, 242–249 (2009).
57. Brainard, D. H. The Psychophysics Toolbox. *Spat. Vis.* **10**, 433–436 (1997).
58. Gramfort, A. et al. MEG and EEG data analysis with MNE-Python. *Front. Neurosci.* **7**, 267 (2013).
59. Lachaux, J. P., Rodriguez, E., Martinerie, J. & Varela, F. J. Measuring phase synchrony in brain signals. *Hum. Brain Mapp.* **8**, 194–208 (1999).
60. Tsolaki, E., Espinoza, R. & Pouratian, N. Using probabilistic tractography to target the subcallosal cingulate cortex in patients with treatment resistant depression. *Psychiatry Res. Neuroimaging* **261**, 72–74 (2017).
61. Fricke, P. et al. Directional leads for deep brain stimulation: technical notes and experiences. *Stereotact. Funct. Neurosurg.* **99**, 305–312 (2021).
62. Fan, X. Biased emotion processing in TRD. *OSF* <https://osf.io/93wf2/> (2023).

Acknowledgements

We thank all patients for their participation and all clinical technicians in the epilepsy monitoring unit for providing support during the research recordings. We thank S. Pasha for his help in data collection in the epilepsy monitoring unit. We thank C. Kovach for his assistance in developing the task. This work was supported by funding from the United States National Institutes of Health (R01-MH127006 (K.R.B.), NIH K01-MH116364 (K.R.B.) and NIH UH3-NS103549 (K.R.B.)).

Author contributions

Writing: X.F., E.B., A.J.W., K.R.B. and M.M. Review and editing: all authors. Data analysis: X.F., Y.Z., R.K.M. and S.E. Methodology: J.A.A., B.A.M., K.R.B. and N.P. Conceptualization: X.F., K.R.B., B.A.M. and W.G. Funding acquisition: K.R.B., W.G., N.P. and S.J.M. Data collection: B.A.M., M.M., B.P., J.X. and C.H. Project administration: V.P. and A.A.

Competing interests

W.G. receives royalties from Nview, LLC and OCDScales, LLC. N.P. is a consultant for Abbott Laboratories and Sensoria Therapeutics. S.J.M. has received consultant fees from Abbott, Almatica Pharma, Beckley Psytech, Biohaven, BioXcel Therapeutics, Boehringer-Ingelheim, Bria Biosciences, Clexio Biosciences, COMPASS Pathways, Delix Therapeutics, Douglas Pharmaceuticals, Engrail Therapeutics, Freedom Biosciences, LivaNova, Levo Therapeutics, Merck, Motif

Neurotech, Neumora, Neurocrine, Perception Neuroscience, Praxis Precision Medicines, Relmada Therapeutics, Sage Therapeutics, Seelos Therapeutics, Signant Health, Sunovion Pharmaceuticals, Xenon Pharmaceuticals, Worldwide Clinical Trials and XWPPharma. S.J.M. has received research support from Boehringer-Ingelheim, Engrail Therapeutics, Merck, Neurocrine and Sage Therapeutics. The other authors declare no competing interests.

Additional information

Extended data is available for this paper at <https://doi.org/10.1038/s44220-024-00238-w>.

Supplementary information The online version contains supplementary material available at <https://doi.org/10.1038/s44220-024-00238-w>.

Correspondence and requests for materials should be addressed to Kelly R. Bijanki.

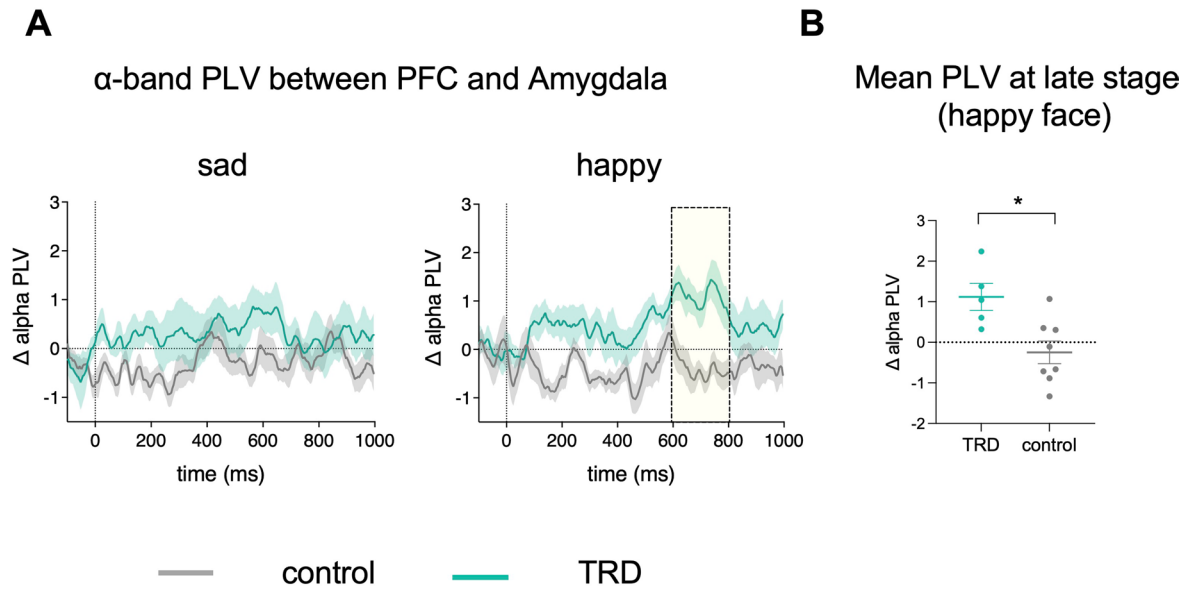
Peer review information *Nature Mental Health* thanks Hideki Azuma, Alena Damborska and the other, anonymous, reviewer(s) for their contribution to the peer review of this work.

Reprints and permissions information is available at www.nature.com/reprints.

Publisher's note Springer Nature remains neutral with regard to jurisdictional claims in published maps and institutional affiliations.

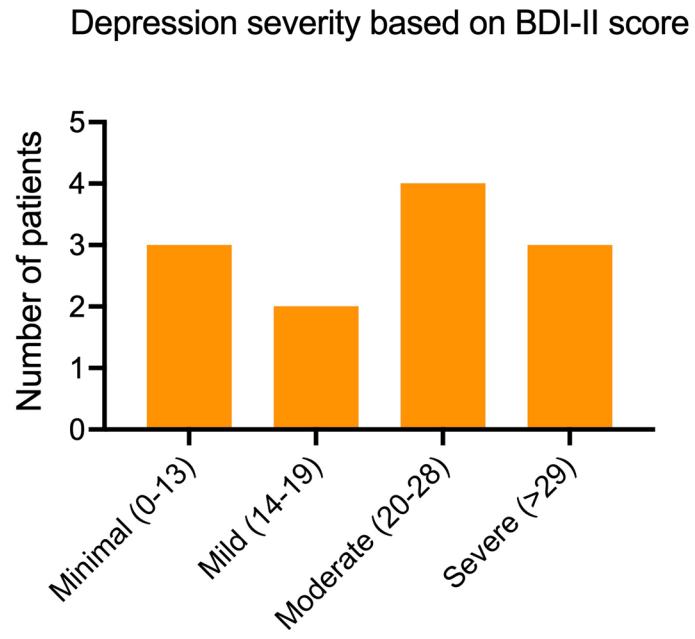
Open Access This article is licensed under a Creative Commons Attribution 4.0 International License, which permits use, sharing, adaptation, distribution and reproduction in any medium or format, as long as you give appropriate credit to the original author(s) and the source, provide a link to the Creative Commons licence, and indicate if changes were made. The images or other third party material in this article are included in the article's Creative Commons licence, unless indicated otherwise in a credit line to the material. If material is not included in the article's Creative Commons licence and your intended use is not permitted by statutory regulation or exceeds the permitted use, you will need to obtain permission directly from the copyright holder. To view a copy of this licence, visit <http://creativecommons.org/licenses/by/4.0/>.

© The Author(s) 2024

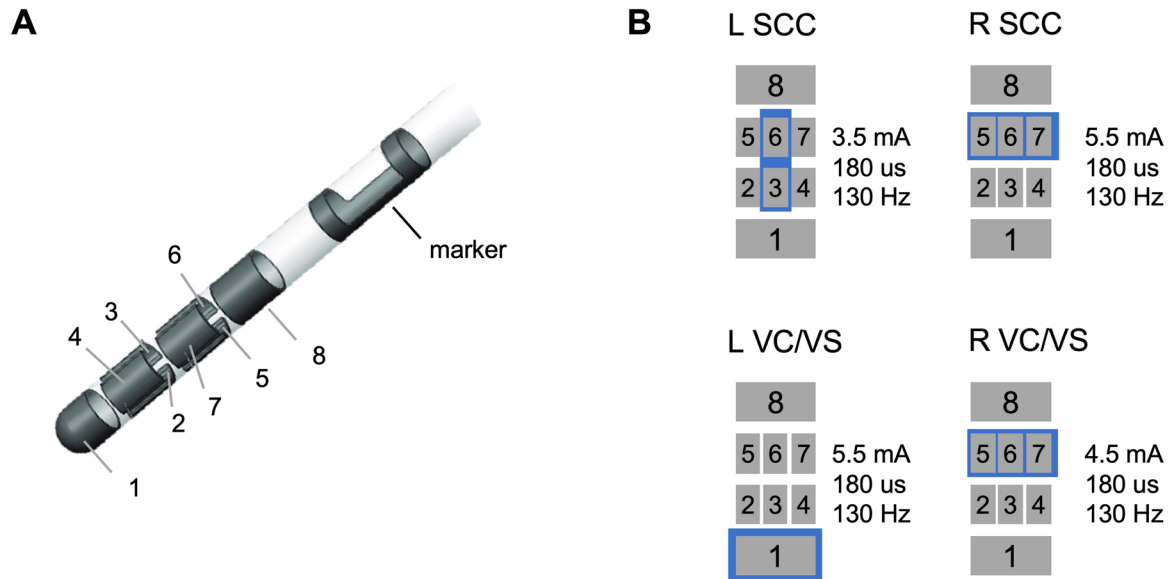


Extended Data Fig. 1 | Connectivity analysis after matching the number of contacts in TRD and control patients. (a) Average time courses (mean \pm SEM) of alpha PLV changes from baseline in TRD (5 patients) and control group (8 patients). Yellow shade area indicates the time window in which responses to each stimulus type (sad and happy faces) are significantly different between

TRD and control group with a cluster threshold of $p < 0.05$. **(b)** During the late stage of happy face processing, TRD patients display stronger PLV between PFC and amygdala than control patients ($t_{11} = 3.094$, $p = 0.0102$). Data are presented as mean values \pm SEM. Each dot means a single participant. * $p < 0.05$ (two-sided unpaired t tests). PLV, phase locking value. $N_{\text{TRD}} = 5$, $N_{\text{control}} = 8$.



Extended Data Fig. 2 | Depression severity based on BDI-II score. BDI-II scores across the 12 epilepsy patients exhibit a distribution from minimal to severe depression.



Boston Scientific directional 8-contact lead

Stimulation parameter sets

Extended Data Fig. 3 | DBS lead and stimulation parameter. (a) Contact arrangement for the Boston Scientific directional 8-contact lead. (b) An example of deep brain stimulation parameter set. The blue squares indicate the combination of DBS contacts through which stimulation was delivered.

Corresponding author(s): Kelly Bijanki

Last updated by author(s): Mar 7, 2024

Reporting Summary

Nature Portfolio wishes to improve the reproducibility of the work that we publish. This form provides structure for consistency and transparency in reporting. For further information on Nature Portfolio policies, see our [Editorial Policies](#) and the [Editorial Policy Checklist](#).

Statistics

For all statistical analyses, confirm that the following items are present in the figure legend, table legend, main text, or Methods section.

- | | |
|-------------------------------------|------------------------------------------------------------------------------------------------------------------------------------------------------------------------------------------------------------------------------------------------------------------------------------------------|
| n/a | Confirmed |
| <input type="checkbox"/> | <input checked="" type="checkbox"/> The exact sample size (n) for each experimental group/condition, given as a discrete number and unit of measurement |
| <input type="checkbox"/> | <input checked="" type="checkbox"/> A statement on whether measurements were taken from distinct samples or whether the same sample was measured repeatedly |
| <input type="checkbox"/> | <input checked="" type="checkbox"/> The statistical test(s) used AND whether they are one- or two-sided
<i>Only common tests should be described solely by name; describe more complex techniques in the Methods section.</i> |
| <input type="checkbox"/> | <input checked="" type="checkbox"/> A description of all covariates tested |
| <input type="checkbox"/> | <input checked="" type="checkbox"/> A description of any assumptions or corrections, such as tests of normality and adjustment for multiple comparisons |
| <input type="checkbox"/> | <input checked="" type="checkbox"/> A full description of the statistical parameters including central tendency (e.g. means) or other basic estimates (e.g. regression coefficient) AND variation (e.g. standard deviation) or associated estimates of uncertainty (e.g. confidence intervals) |
| <input type="checkbox"/> | <input checked="" type="checkbox"/> For null hypothesis testing, the test statistic (e.g. F , t , r) with confidence intervals, effect sizes, degrees of freedom and P value noted
<i>Give P values as exact values whenever suitable.</i> |
| <input checked="" type="checkbox"/> | <input type="checkbox"/> For Bayesian analysis, information on the choice of priors and Markov chain Monte Carlo settings |
| <input checked="" type="checkbox"/> | <input type="checkbox"/> For hierarchical and complex designs, identification of the appropriate level for tests and full reporting of outcomes |
| <input checked="" type="checkbox"/> | <input type="checkbox"/> Estimates of effect sizes (e.g. Cohen's d , Pearson's r), indicating how they were calculated |

Our web collection on [statistics for biologists](#) contains articles on many of the points above.

Software and code

Policy information about [availability of computer code](#)

Data collection Intracranial EEG data were recorded using Cerebus data acquisition system (Blackrock Neurotech). DBS leads (Cartesia, Boston Scientific) and sEEG electrodes (Depthalton, PMT Corporation) were implanted using a Robotic Surgical Assistant (ROSA, Zimmer Biomet).

Data analysis Intracranial EEG data were analyzed using MNE-python v1.6 (<https://mne.tools/stable/index.html>) and MATLAB R2023a. Electrodes were localized by co-registration of pre-surgery anatomical T1 MRI scans and post-implantation CT scans using FreeSurfer Version 6 (<https://surfer.nmr.mgh.harvard.edu>). Electrode positions were manually marked using Biolumage Suite. iELVis was used to overlay electrode location into the MRI. The experiment was programmed in MATLAB R2019a, using Psychtoolbox-3. The data that support the key findings and codes used to analyze the data are available on Open Science Framework (<https://osf.io/93wf2/>).

For manuscripts utilizing custom algorithms or software that are central to the research but not yet described in published literature, software must be made available to editors and reviewers. We strongly encourage code deposition in a community repository (e.g. GitHub). See the Nature Portfolio [guidelines for submitting code & software](#) for further information.

Data

Policy information about [availability of data](#)

All manuscripts must include a [data availability statement](#). This statement should provide the following information, where applicable:

- Accession codes, unique identifiers, or web links for publicly available datasets
- A description of any restrictions on data availability
- For clinical datasets or third party data, please ensure that the statement adheres to our [policy](#)

The data that support the key findings are available on Open Science Framework (<https://osf.io/93wf2/>). The access links are listed in the "Data availability" section.

Research involving human participants, their data, or biological material

Policy information about studies with [human participants or human data](#). See also policy information about [sex, gender \(identity/presentation\), and sexual orientation](#) and [race, ethnicity and racism](#).

Reporting on sex and gender	Data were obtained from twelve epilepsy patients (7 Female, 5 Male, Age 19-57) and five treatment-resistant depression (TRD) patients (3 Female, 2 Male, Age 32-56).
Reporting on race, ethnicity, or other socially relevant groupings	The ethnicity of our epilepsy patients are as follows: 67% White, 8% Asian, 17% African American and 8% Unknown. The ethnicity of our TRD patients are as follows: 20% Hispanic and 80% White.
Population characteristics	Data were obtained from twelve epilepsy patients (7 Female, 5 Male, Age 19-57) and five treatment-resistant depression (TRD) patients (3 Female, 2 Male, Age 32-56). See Method section for more details.
Recruitment	Epilepsy patients undergoing iEEG monitoring for seizure localization were recruited for this research study based on their willingness and capability to participate. All five treatment-resistant depression patients involved in the clinical trial (ClinicalTrials.gov Identifier: NCT03437928) were recruited and consented to participate this study. The patients get paid \$100 per day.
Ethics oversight	All the experiments in this paper involved epilepsy patients and TRD patients were approved by the Institutional Review Board at Baylor College of Medicine (IRB: H-43036, IRB: H-18112). Written informed consent was obtained from each participant.

Note that full information on the approval of the study protocol must also be provided in the manuscript.

Field-specific reporting

Please select the one below that is the best fit for your research. If you are not sure, read the appropriate sections before making your selection.

- Life sciences Behavioural & social sciences Ecological, evolutionary & environmental sciences

For a reference copy of the document with all sections, see [nature.com/documents/nr-reporting-summary-flat.pdf](https://www.nature.com/documents/nr-reporting-summary-flat.pdf)

Behavioural & social sciences study design

All studies must disclose on these points even when the disclosure is negative.

Study description	We obtained continuous intracranial electroencephalography (iEEG) recordings in the amygdala and prefrontal cortex from 12 epilepsy patients and 5 treatment-resistant depression patients. They were asked to do an affective bias task in which happy and sad faces were evaluated. Based on these data, we examined the brain mechanisms underlying the emotion processing bias in people with treatment-resistant depression. This study is quantitative.
Research sample	Twelve epilepsy patients (7 Female, 5 Male, Age 19-57) and five treatment-resistant depression (TRD) patients (3 Female, 2 Male, Age 32-56) were involved. All our TRD patients have a DSM-5 diagnosis of MDD as their primary diagnosis and failure to respond to a minimum of four adequate depression treatments from at least two different treatment medication categories (SSRI, SNRI, TCA, MAOI, etc.). Epilepsy patients with electrodes implanted for clinical purpose were used as control group in this study because it is almost the only opportunity to obtain intracranial EEG recordings in nearly healthy humans. These samples are considered as representative.
Sampling strategy	Epilepsy patients with electrodes implanted for clinical purpose were asked whether they were willing to participate research before surgery. The epilepsy patients have at least one electrode in PFC or amygdala were involved in this study. TRD patients participated the clinical trial (ClinicalTrials.gov Identifier: NCT03437928) were asked whether they were willing to participate research. All TRD patients were involved in this study as long as they can provide consent form and were happy to participate. The sample size of TRD is 5 because 6 TRD patients were recruited for the clinical trial and one of them did not provide meaningful data due to the recording

	problems. The sample size of control group (epilepsy patients) is 12 because we need to match the number of contacts in the two groups.
Data collection	TRD patients undergo sEEG research for ten days in the epilepsy monitoring unit (EMU) and they performed the affective bias task twice after surgical implantation, at day 1 or day 2 (before DBS parameter exploration) and day 8 or day 9 (after DBS parameter exploration). Epilepsy patients completed the task during their in-patient stay (at least 2 hours after any seizure activity was detected). Intracranial EEG data were recorded during affective bias task using Cerebus data acquisition system (Blackrock Neurotech). Research coordinators and clinical technicians were present during the experiment. People who collected the data (B.A.M., M.M., B.P., J.X., C.H.) were blinded to the study hypothesis.
Timing	The data has been collected over the course of 3 years from treatment-resistant depression patients (from March 2020 to May 2023), and 2 years from epilepsy patients (from March 2021 to April 2023).
Data exclusions	Trials with obvious wrong click (1.5% in control/epilepsy; 1.4% in TRD) were excluded (for example, 100% happy faces were labeled very sad), which indicated that the patients were distracted from doing the task.
Non-participation	Only patients who provided written consent and completed the task were involved in this study.
Randomization	Participants completed three alternating happy and sad blocks. The order of happy and sad blocks was counterbalanced across participants. In each block, the sequence of neutral, 10%, 30%, 50%, and 100% intensity trials are randomly arranged.

Reporting for specific materials, systems and methods

We require information from authors about some types of materials, experimental systems and methods used in many studies. Here, indicate whether each material, system or method listed is relevant to your study. If you are not sure if a list item applies to your research, read the appropriate section before selecting a response.

Materials & experimental systems

n/a	Involved in the study
<input checked="" type="checkbox"/>	<input type="checkbox"/> Antibodies
<input checked="" type="checkbox"/>	<input type="checkbox"/> Eukaryotic cell lines
<input checked="" type="checkbox"/>	<input type="checkbox"/> Palaeontology and archaeology
<input checked="" type="checkbox"/>	<input type="checkbox"/> Animals and other organisms
<input type="checkbox"/>	<input checked="" type="checkbox"/> Clinical data
<input checked="" type="checkbox"/>	<input type="checkbox"/> Dual use research of concern
<input checked="" type="checkbox"/>	<input type="checkbox"/> Plants

Methods

n/a	Involved in the study
<input checked="" type="checkbox"/>	<input type="checkbox"/> ChIP-seq
<input checked="" type="checkbox"/>	<input type="checkbox"/> Flow cytometry
<input checked="" type="checkbox"/>	<input type="checkbox"/> MRI-based neuroimaging

Clinical data

Policy information about [clinical studies](#)

All manuscripts should comply with the ICMJE [guidelines for publication of clinical research](#) and a completed [CONSORT checklist](#) must be included with all submissions.

Clinical trial registration	NCT03437928
Study protocol	The full trial protocol can be assessed through contacting the study's principal investigator, whose information can be found in ClinicalTrials.gov. The details of study protocol were also described in the article "Deep Brain Stimulation for Depression Informed by Intracranial Recordings" (https://doi.org/10.1016/j.biopsych.2021.11.007).
Data collection	Boston Scientific's Vercise™ DBS system was used in this clinical trial. This study was performed at Houston (Baylor College of Medicine) and Dallas (University of Texas Southwestern). The status is Recruiting in Dallas and Active, not recruiting in Houston. Study start at 2019-8-20 and will be end at 2025-9-19. 12 patients will be enrolled in total by the end of trial.
Outcomes	The outcome measure is Changes in depressive symptoms. Response will be defined as 50% decrease in Montgomery-Asberg Depression Rating Scale (MADRS) from baseline. The range is from 0 to 60 and a score higher than 20 indicates moderate to severe depression. Time frame is 54 to 60 months.

Plants

Seed stocks

Report on the source of all seed stocks or other plant material used. If applicable, state the seed stock centre and catalogue number. If plant specimens were collected from the field, describe the collection location, date and sampling procedures.

Novel plant genotypes

Describe the methods by which all novel plant genotypes were produced. This includes those generated by transgenic approaches, gene editing, chemical/radiation-based mutagenesis and hybridization. For transgenic lines, describe the transformation method, the number of independent lines analyzed and the generation upon which experiments were performed. For gene-edited lines, describe the editor used, the endogenous sequence targeted for editing, the targeting guide RNA sequence (if applicable) and how the editor was applied.

Authentication

Describe any authentication procedures for each seed stock used or novel genotype generated. Describe any experiments used to assess the effect of a mutation and, where applicable, how potential secondary effects (e.g. second site T-DNA insertions, mosaicism, off-target gene editing) were examined.